Journal of Applied Polymer Science

Microwave-assisted chemical synthesis of conducting polyindole: Study of electrical property using Schottky junction

Madhu Tiwari, Ashish Kumar, Harshit Sunil Umre, Rajiv Prakash
School of Materials Science and Technology, Indian Institute of Technology, Banaras Hindu University, Varanasi 221005, India
Correspondence to: R. Prakash (E-mail: rajivprakash12@yahoo.com)

ABSTRACT: A facile and rapid enhanced microwave-assisted route for one-pot synthesis has been developed to polymerize indole moiety using two different oxidizing agents for 60 s exposure at 30 ± 1°C. As-synthesized conducting polyindoles, obtained by varying the synthesis process and oxidant, have been well characterized by various techniques. UV–vis, FT-IR, and NMR have been used for their structural analysis while gel permeation chromatography, thermogravimetric analysis, and conductivity measurement to evaluate their enhanced properties and to perform a comparative study. Morphological texture of polyindole synthesized via different techniques has studied by scanning electron microscopy analysis. PIn synthesized by KIO_3 (microwave synthesis) exhibit interconnecting texture which may be due to high level of supersaturation of solution under the influence of microwave irradiation. Thereafter, electrical property of spin-coated thin film of polyindole is examined using four probe method and Al metal/semiconducting material Schottky junction. Microwave-assisted polymer shows better performance for Schottky devices due to difference in charge transport, morphological texture, and distribution of M_n. The PIn synthesized via microwave irradiation with better charge transport across the metal/polymer interfaces shows the potential of this technique for synthesis of such polymers with enhanced electronic properties. © 2015 Wiley Periodicals, Inc. J. Appl. Polym. Sci. **2015**, *132*, 42192.

KEYWORDS: applications; conducting polymers; microwave synthesis; synthesis and processing

Received 2 October 2014; accepted 8 March 2015
DOI: 10.1002/app.42192

INTRODUCTION

Microwave-assisted synthesis has recently been explored as an important technique for synthesis of materials. This nonconventional synthetic strategy has displayed broad applications to accelerate the course of many organic reactions in an effective way. It offers higher reaction rates, better selectivity, shorter reaction time, high yield production, lower quantities of side products as a result, facile work-up and purification of products as compared with conventional methods.[1,2] It is reported that microwave involves dielectric heating which couples directly with the microwave absorbing polar solvent molecules that are present in the reaction mixture and transfer energy selectively leading to a fast rise in temperature, rapid reactions, cleaner chemistry, and nucleation of the polymeric material.[3] There are two fundamental mechanisms, dipole rotation and ionic conduction, that are reported for the transfer of energy from microwaves to the substance. Thus, it can facilitate mass production in a very short time frame with little energy cost and forms an intimate contact between reacting species which is crucial for the formation of electronic interactions and interelectron transfer at the interface. This is because these electromagnetic waves directly interact with the full volume of material at a molecular level via dipolar interactions thus penetrating through the material to deliver the energy and produce cubical heating of the material. Consequently, it is possible to achieve a rapid volumetric and uniform heating of materials.[4,5] Enhanced microwave synthesis has potential to deal with the issue of product yields, reaction time, side products, and the product purities. By applying microwave irradiation along with external cooling the reaction vessel, a steady amount of energy can be transferred to reaction mixture, while maintaining a constant temperature (±1°C). In this way, a precise nonthermal effects of microwave irradiation can be magnified in controlled way.[6,7]

Nowadays researchers have started microwave-assisted synthesis approach for the preparation of various compounds *viz.* spiroorthoester, phenyl oxazoline, polymers (poly 9,9-dihexylfluorene, polyesters), and polymer composites/copolymers.[8–10] On the other hand, with the advent of conducting polymers, the researchers are exploring the potential of these materials as a substitute of conventional inorganic semiconductors in area of

Additional Supporting Information may be found in the online version of this article.

sensors, catalysis, optoelectronic devices mostly due to their magnetic, optical, and electronic properties, which are analogous to metals while retaining the processability and flexibility of conventional polymers. This is due to easy synthesis, easy modification, and good redox properties.[11,12] A variety of electronic and optoelectronic devices based on conducting polymers have been formulated and used in civil and military industries. These devices consist of polymer-based Schottky diodes, thin-film field effect transistor, and tunnel diodes in metal-semiconductor-insulator Schottky gate form, photovoltaic devices, and light-emitting diodes.[13–16]

Conducting polymers and its composite have been synthesized in various ways chemically and electrochemically at room temperature. For example, conducting polymers like polyaniline, polypyrrole, polycarbazole, and its composite have been synthesized using multiwalled carbon nanotubes,[17] metal oxide,[18,19] metal nanoparticles,[20–23] and its properties has been studied. A part of these, polyindole (PIn) is one of the heterocyclic conducting polymers having excellent electrical properties with the advantage of straightforward synthesis, good environmental stability, and high processability. It is regarded as an excellent material for diversified applications due to combined property of polyphenylene and polypyrrole, good redox properties, easy synthesis both by chemical and electrochemical polymerization methods. Similar to other conducting polymers polyindole and its derivatives have recently been used for a variety of applications such as diodes, sensors, catalysts, charge storage devices, fuel cell batteries, etc.[24] Literature survey reveals that conducting polymers like polyaniline, polycarbazole, and polythiophene have been synthesized by microwave irradiation.[25–28] However, the microwave-assisted synthesis of polyindole and its utilization as active material in electronic devices has not been explored so far. That is why we are motivated to give a contribution in this context. In this article, we report facile one pot synthesis of PIn using microwave irradiation and development of organic Schottky diode based on polyindole as an active material with a configuration of Al/PIn/Indium tin oxide (ITO)-coated glass (Al/PIn/ITO). There are four different sets of devices that are constructed in separate batches using polyindole synthesized by two different oxidizing agents—ammonium persulfate (APS) and potassium iodate (KIO_3) via conventional (*in situ* polymerization for 24 h) and microwave techniques (polymerization for 60 s under microwave irradiation). Our main aim is to overcome the challenges of lower reaction rates thus causing longer reaction time, and unproductive recyclability that are encountered with the conventional method for polymerization of indole and also improvement in the materials through the synthesis routes for electronic applications.

EXPERIMENTAL

Materials

Indole was purchased from Aldrich. Ammonium persulfate ($(NH_4)_2S_2O_8$) was purchased from HiMedia, India. Ethanol, dichloromethane, *n*-hexane, potassium iodate (KIO_3), nitric acid (HNO_3), and hydrochloric acid (HCl) were purchased from Merck, India. The glasswares used in the synthesis of polymer were cleaned with freshly prepared aqua regia (3 : 1, HCl/HNO_3) and rinsed comprehensively with ultrapure water (Merck, India). ITO glass or metal electrodes coated with polymer were properly washed and dried before device fabrication or other characterization.

Microwave and Conventional Synthesis of PIn

Four sets of PIns were synthesized by varying oxidants and polymerization condition in aqueous phase using ethanol as co-solvent. In every set of experiment 1 : 2 mole ratio of indole : oxidant was chosen and was synthesized by following procedure. 1.0 g indole was dissolved in 500 μL of ethanol and then digested slowly into 100 mL of 0.1*N* HCl under constant stirring and the mixture was stirred for 30 min. After that 3.896 g $(NH_4)_2S_2O_8$ (dissolved in 100 mL 0.1*N* HCl) was added drop wise in indole solution. The solution rapidly turned into light green as ammonium per sulfate dropped. This reaction mixture was kept in microwave radiation (microwave parameters: temperature: $(30 \pm 1)^\circ$C, frequency: 300 MHz; energy output: 800; energy input: 1200) for 60 s. Polymerization proceeded with change in color from light green to dark green followed by precipitation. This dark green precipitate was filtered, and then washed by dissolving in ethanol, dichloromethane, and deionized water repeatedly to remove monomer/oligomer and unreacted oxidant. Finally, it was dried under vacuum and preserved for further experimentation.

Similar procedure was adapted for indole polymerization via conventional method using APS as oxidant for 24 h. In addition, two more PIn samples were synthesized via microwave irradiation using KIO_3 by the means of similar procedure as stated above. However, at final stage, as-synthesized PIn was washed (repeatedly by suspending in ethanol followed by dichloromethane to remove monomer and *n*-hexane to remove residual of iodine) and dried in vacuumed desiccator.

Instrumentation

As-synthesized PIn was characterized and compared for their structural, morphological, thermal analysis, and conductivity measurements by various characterization tools. Fourier transform-infrared (FT-IR) spectra in KBr pellets were recorded from 4000 to 400 cm^{-1} with FT-IR spectrometer (Nicolet-6700). UV-Vis absorption spectra were recorded using Perkin Elmer Lambda-25 spectrophotometer (obtained under DAAD Instrument grant Germany) by using a quartz cuvette having optical path length of 1 cm. ^{1}H-NMR spectra of the resulting polymers were recorded on a JEOL AL300 FTNMR (300 MHz) in $CDCl_3$ solvent and are reported in parts per million (δ) from residual solvent peak. Thermogravimetric analysis (TGA) was performed on Mettler Tuldeo (TGA/DSC 1 STARE System, Switzerland) at the rate of 20°C min^{-1} in nitrogen atmosphere. The number-average molecular weight (M_n), weight average molecular weight (M_w) and polydispersity index (PDI = M_w/M_n) were determined by Youglin ACME 9000 gel permeation chromatography (GPC) in DMF at 40°C with flow rate 0.5 mL/min [PL gel 5 μm 10E 4 Å columns (300 7.5 mm)] connected in series to Younglin ACME 9000 Gradient Pump and a Younglin ACME 9000 RI detector. Scanning electron microscopy (SEM) was performed on Curl Zeiss, Supra-40, Germany at operating voltage 5 kV for morphological analysis. PIn polymerization under microwave radiation was performed on microwave synthesis system (MAS-II Sineo

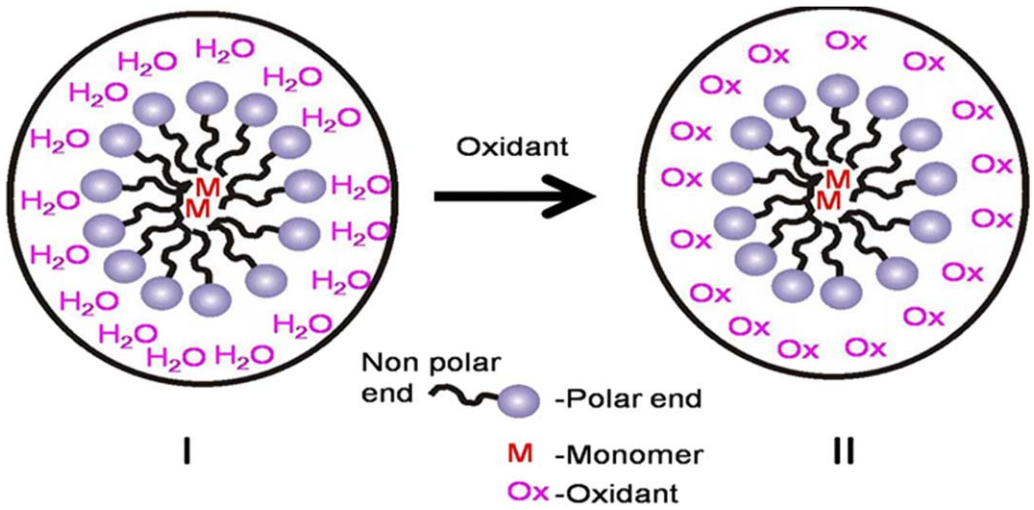

Scheme 1. Schematic representation of monomer based micelle formation in ethanol-in-water system (I) before and (II) after addition of aqueous oxidant. [Color figure can be viewed in the online issue, which is available at wileyonlinelibrary.com.]

microwave synthesis workstation, China) at (30 ± 1)°C at frequency 300 MHz. Current–voltage (*I–V*) measurements of devices ITO/PIn/Al structure were carried out with source meter of Keithley (model 2612A) at room temperature (27°C) in air under dark condition. Conductivity measurements were performed on CMT-SR2000N Sheet Resistance/Resistivity measurement System, Korea. Atomic force microscope (AFM) images were observed using AFM-STM, model PRO 47, NT-MDT, Russia. The sample preparation step for AFM, conductivity measurement by four probe method and device fabrication was same (as discussed later in Device Fabrication section).

RESULTS AND DISCUSSION

Ethanol containing dissolved indole, establishes metastable spherical micelles (ethanol in water) when allowed to digest in water under constant stirring condition as shown in Scheme 1. These micelles act as soft template for construction of specific sized polymer.[29,30] It is reported that PIn exists in hollow macrospherical form when polymerization reaction occurs along the wall of stable micelles in presence of oxidizing agents for 24 h. However, variation in morphology depends on the stability of the micelles formed, method, and oxidizing agents used for polymerization.[29] In the present case, micelles consisting of indole moiety are polymerized under microwave irradiation using two different oxidizing agents. In polymerization process polar solvent mixture (ethanol + water) acts as the principal microwave absorber and can therefore be selectively heated (between ethanol-water mixture and indole) near the vicinity of micelles. This leads to the one pot nucleation of polymeric chains in presence of oxidants in just a few seconds.[30] Differences in the morphological textures of PIn formed conventionally and microwave irradiation routes are due to different level of supersaturation as discussed by SEM latter.

Structural Analysis

PIn synthesized from various methods is compared by FT-IR as shown in Figure 1. The major characteristics peaks are assigned for the association of indole monomers together through two to three linkage as reported earlier[31,32] and details are given in Table I. The vibrational peaks are almost similar in all cases as the monomeric linkage for polymer growth is same even on changing the oxidants and synthesis conditions. As in case of PIn (synthesized conventionally by APS), the strong vibrational peak at 748 cm^{-1} is assigned due to out of plane deformation of C—H bond of benzene ring in indole moiety. Vibration peak at 1450 cm^{-1} corresponds to stretching mode of benzene rings indicating that benzene ring (in indole monomer) is not the polymerization site. Vibration peak at 3299 cm^{-1} (due to N—H stretching vibrations), together with vibration peak near 1567 cm^{-1} (due to N—H deformation vibrations), are clear indication for the existence of N—H bond (in pyrrole ring) even in the PIn backbone. This observation establishes that N site is not the polymerization site and feasible polymerization

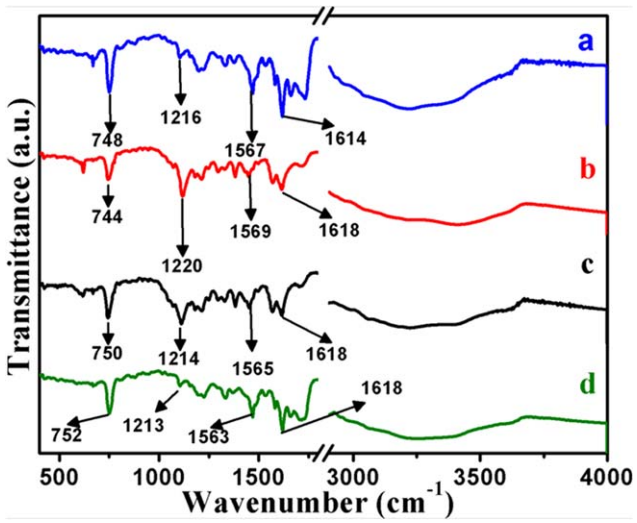

Figure 1. FT-IR of PIn formed by APS (a) and KIO_3 (b) (conventional synthesis), PIn formed by APS (c), and KIO_3 (d) (microwave synthesis). [Color figure can be viewed in the online issue, which is available at wileyonlinelibrary.com.]

Table I. Vibrational Peak (in cm^{-1}) of PIn Observed by FT-IR Analysis

S. No.	PIn formed by APS (conventional synthesis)	PIn formed by KIO_3 (conventional synthesis)	PIn formed by APS (microwave synthesis)	PIn formed by KIO_3 (microwave synthesis)	Assignments
1	748	744	750	752	C—H bond of benzene ring
2	1118	1103	1110	1103	C—N vibration
3	1216	1220	1214	1213	N—H bending vibration
4	1450	1469	1452	1471	Stretching mode of benzene ring
5	1567 (very weak)	1569 (very weak)	1565 (very weak)	1563 (very weak)	N—H deformations and vibration modes of $-C_2=C_3-$ aromatic bonds
6	1614	1618	1618	1618	-C=C- stretching vibrations
7	3299	3291	3290	3251	Stretching vibrations of N—H bond

take place at 2- and 3-positions. The characteristics vibrations in the frequency range of 1100 to 1600 cm^{-1} are assigned due to vibrations of benzene rings. Similarly PIn formed via other routes, have almost similar vibrational peaks. The slight variation in their vibrational peak positions may be due to different ease of conjugation length.[33] This observation reveals that the mechanism of PIn polymerization is same in all cases.

The indole polymerization mechanism for PIn formation is further supported by ^{1}HNMR. The ^{1}HNMR of PIn synthesized via various methods are shown in Figure 2. As illustrated from Figure 2(a), PIn synthesized by APS conventionally consists of characteristics peaks for H_4 at $\delta = 9.06$ ppm, H_5 at $\delta = 6.64$–7.72 ppm, H_6 at $\delta = 6.7$ ppm to 7.71 ppm and H_7 at $\delta = 7.72$ ppm to 7.85 ppm of benzene ring in indole unit.[34] The chemical shift of peak from $\delta = 10.74$ ppm to 11.0 ppm is due to the presence of H_1 in N—H group[35] which is influenced by H_7 of benzene ring. These peaks can also be observed in the PIn synthesized via other methods, indicating similar mode of indole polymerization (2, 3 position) even varying the oxidants and synthesis method [cf. Figure 2(b–d) with Figure 2(a)]. The broadening in ^{1}HNMR spectra for all synthesized PIn is expected due to wide distribution of molar masses (chain length) causing self-aggregation of polymeric molecules in analyte which is verified by GPC also (as discussed latter).[36]

Similarly, different functionalities in PIn synthesized via various methods were further cross-checked by UV-Vis analysis examined in DMSO solution as shown in Figure 3. PIn synthesized by APS conventionally [as shown in Figure 3(a-I)] exhibit three peaks at 310, 360, and 550 nm. First and second peak correspond to π-π^* transition and n-π^* transition while the third one is due to polaronic excitations (effect of doping).[37] On the other hand, PIn synthesized by microwave (using APS) consists of similar absorption peak and almost same position [cf. Figure 3(a-I) and (a-II)]. Herein in case of PIn synthesized conventionally, the polaronic band at 550 nm [observed at higher wavelength as shown in inset Figure 3(a)] gets blue shift to 450 nm in case of the PIn synthesized by microwave irradiation indicating decrease in conjugation length (or enhancements in band gap).[38] However, in case of PIn synthesis using KIO_3 (by either synthesis method) this polaronic band is constant and observed at 460 nm [as shown in inset of Figure 3(b)], indicating almost similar conjugation length.

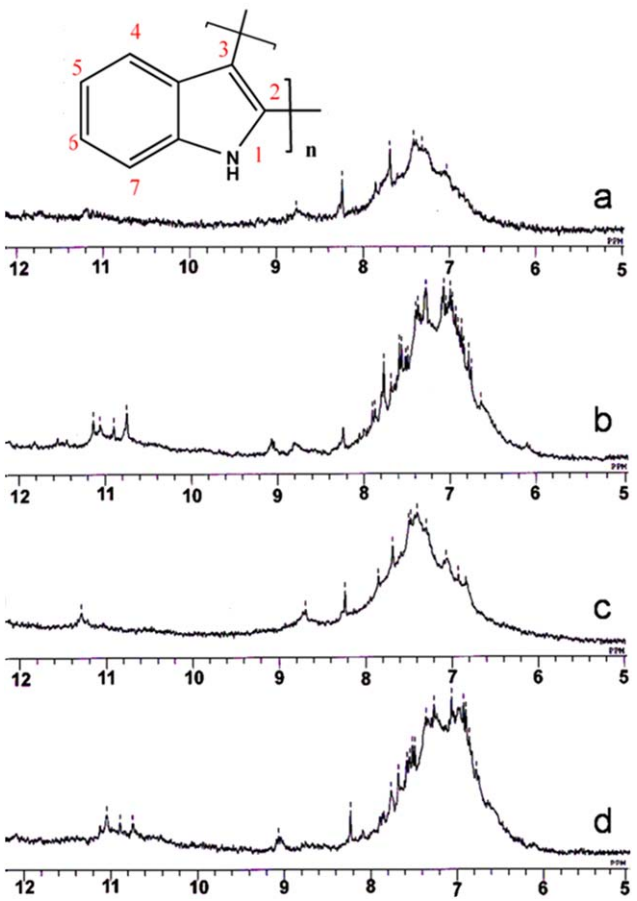

Figure 2. ^{1}HNMR of PIn formed by APS (a) and KIO_3 (b) (conventional synthesis), PIn formed by APS (c), and KIO_3 (d) (microwave synthesis). *x*-axis represents chemical shift (in ppm) and *y*-axis represents signal intensity (a.u.). Inset shows chemical structure of PIn. [Color figure can be viewed in the online issue, which is available at wileyonlinelibrary.com.]

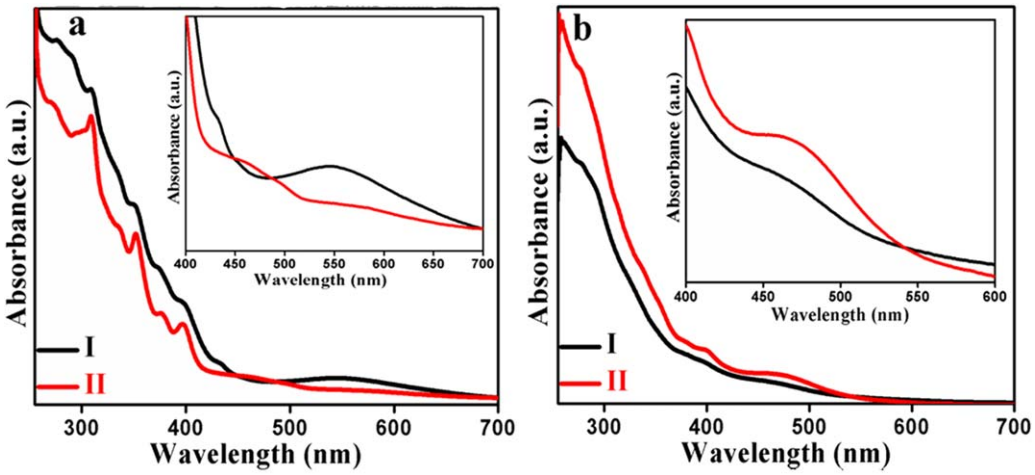

Figure 3. UV-Vis of PIn formed by (a) APS and (b) KIO_3 by conventional synthesis (I) and by microwave synthesis (II). Inset shows the excitation due to doping. [Color figure can be viewed in the online issue, which is available at wileyonlinelibrary.com.]

Morphological Analysis

Micro-textures of PIns are analyzed by SEM as shown in the Figure 4 (aliquots of dispersed PIn is directly taken over carbon coated stab for SEM). SEM images of PIn synthesized by APS using either methods (conventional and microwave method) consist of irregular hollow globular-shaped morphology with almost similar sizes [cf. Figure 4(a,c)]. In case of PIn, synthesized conventionally by KIO_3 [cf. Figure 4(b)], has also globular morphology but relatively smaller in size compared with PIn synthesized by APS using either synthesis methods [cf. Figure 4(a,c)]. However, this globular shaped texture has collapsed together and provides well-defined interconnections between individual globules in case of PIn synthesized by KIO_3 using microwave synthesis method [cf. Figure 4(a,d)]. These interconnections are probably expected due to sufficiently high level of supersaturation of solution using KIO_3 under the influence of microwave irradiation thus causing heterogeneous nucleation of PIn. Supersaturation is directly related to activation energy, probability of molecular impacts, and thus nucleation process. When the supersaturation level decreases the activation energy gets elevated and spontaneous heterogeneous nucleation occurs which favored agglomerated structures in the materials.[39] Probably in our case the interconnecting structure is the major reason for the better electrical properties and device performance

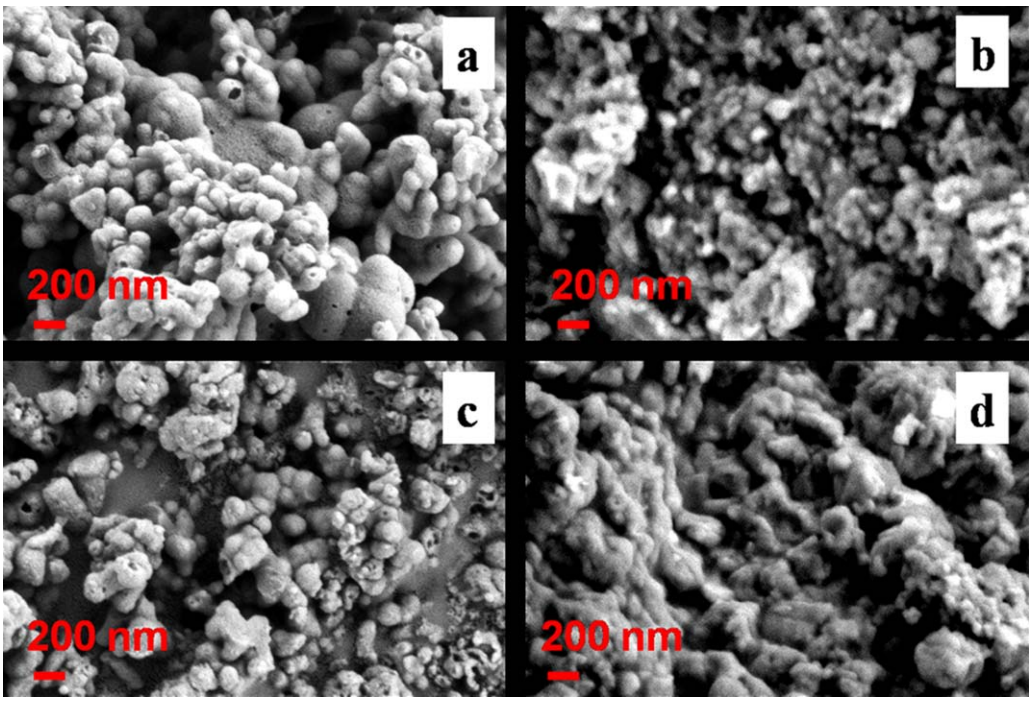

Figure 4. SEM of PIn formed by APS (a) and KIO_3 (b) (conventional synthesis), PIn formed by APS (c), and KIO_3 (d) (microwave synthesis) at magnification 100 KX.[Color figure can be viewed in the online issue, which is available at wileyonlinelibrary.com.]

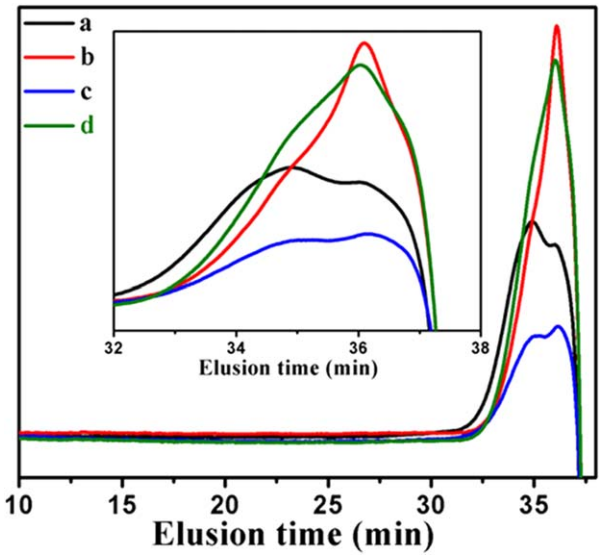

Figure 5. GPC of PIn formed by APS (a) and KIO_3 (b) (conventional synthesis), PIn formed by APS (c), and KIO_3 (d) (microwave synthesis). Inset shows enlarge view of curve. [Color figure can be viewed in the online issue, which is available at wileyonlinelibrary.com.]

as discussed later. The difference in morphology may be due to the different extent of reaction kinetics of oxidants. The morphology of as synthesized has also been analyzed by AFM as shown in Supporting Information Figure S3. We observed almost same morphologies as in the case of SEM.

Molecular Weight Determination

The molecular distributions of PIn synthesized by various methods are determined by GPC (limited for DMF soluble parts of the PIn) as shown in Figure 5 with their various parameters as summarized in Table II. As illustrated from chromatographic results, M_n of dominant fraction is located around 950 and 1500 for PIn synthesized conventionally using APS and KIO_3, respectively [as shown in Figure 5(a,b)], while 1450 and 1550 for PIn synthesized by APS and KIO_3 via microwave radiation, respectively [as shown in Figure 5(c,d)]. Sharp peaks are observed for PIn obtained using oxidizing agent KIO_3 indicating a narrow distribution of M_n while the minuscule humps present for PIn obtained using oxidizing agent APS (as shown in inset of Figure 5) are due to fragmentation of polymeric chains and traces of lower molecular weight polymeric fragments (i.e. wide range distribution of M_n).[40]

Table II. M_n and PDI of PIns Observed by GPC

Synthesis method	Oxidizing agent	Mn (g mol^{-1})	PDI
Conventional	APS	950	1.23
	KIO_3	1500	1.16
Microwave	APS	1450	1.28
	KIO_3	1550	1.19

where M_n is the number average molecular weight and polydispersity index (PDI).

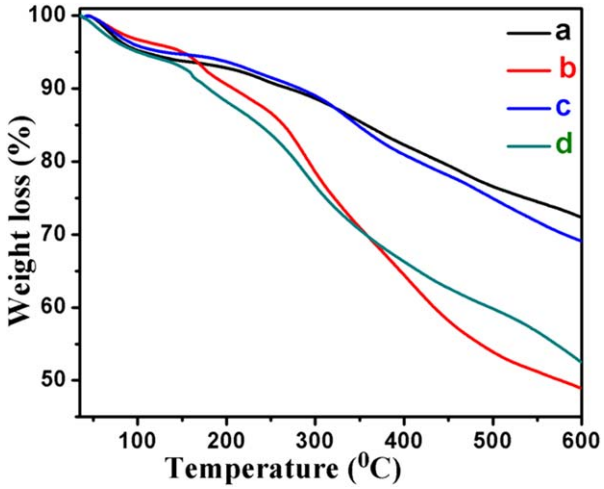

Figure 6. TGA of PIn formed by APS (a) and KIO_3 (b) (conventional synthesis), PIn formed by APS (c), and KIO_3 (d) (microwave synthesis). [Color figure can be viewed in the online issue, which is available at wileyonlinelibrary.com.]

Thermogravimetric Analysis

TGA of PIns synthesized by various methods are carried out under nitrogen atmosphere to examine their thermal stability (as shown in Figure 6). TGA curves exhibited a gradual degradation of all PIn on increasing the temperature. The weight loss observed below 100°C is due to loss of water molecules or moisture present in polymeric matrix.[35] The thermal stability of PIn synthesized by APS (either technique) is slightly better than that of PIn synthesized by KIO_3. This is due to wide range molecular weight distribution of PIn synthesized by APS in which the longer polymeric chains may be grasped together by smaller chains. That is why PIn synthesized by APS shows degradation of about 67% at 600°C whereas PIn synthesized by KIO_3 shows same degradation at 340°C. Thermal behavior of PIns is also analyzed by DTA (as is shown in Supporting Information Figure S1). From this study we observed that degradation of PIns is exothermic in nature from 100°C to 600°C.

The kinetic parameters such as activation energy (E_a) and regression value of PIn thermal decomposition are evaluated using Broido plot[41] (as shown in Supporting Information Figure S2). As illustrated from the table, E_a for decomposition of PIn synthesized by microwave radiation is relatively high in each case showing larger energy barrier for PIn decomposition.

Device Fabrication

A sandwich cell of Al/PIn/ITO was fabricated by constructing PIn films of almost similar thickness over ITO coated glass plate followed by assembling Al metal thin dots over PIn coated ITO-glass plate using the thermal vacuum evaporation method as shown in Scheme 2 in which electrical connection is built via lead L_1 and L_2. In each device PIn film is prepared over ITO-glass by spin coating (deposition of 10 µL at 1200 rpm for 300 s). Thickness of PIn films are about 500 nm observed by AFM (tapping mode) (as shown in Supporting Information Figure S3). The size distribution of PIns formed by different techniques are analyzed by AFM images and shown in Supporting

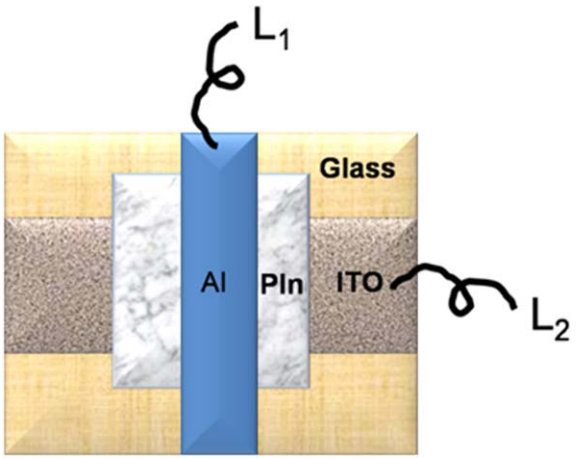

Scheme 2. Schematic representation of device (top view) by sandwiching Al/PIn/ITO layer over glass plate. [Color figure can be viewed in the online issue, which is available at wileyonlinelibrary.com.]

Information Figure S4. The average size of polymeric particles is 175 nm. The Al/PIn/ITO device was not sealed up from attack of moisture and oxygen, but kept in a vacuum desiccator for further characterization.

The electronic properties of the devices, Al/PIn/ITO are investigated by current density-voltage (J–V) measurement at room temperature (27°C) in air under dark conditions. The deviation of current density values from typical features at different applied voltages for four sets of devices fabricated in the lab are shown in Figure 7. As illustrated from this Figure 7, the J–V characteristic of Al/PIn/ITO device exhibits superior rectification behavior for PIn synthesized by microwave radiation compared with PIn synthesized conventionally [cf. Figure 7(b,d) with Figure 7(a,c)]. At the same time, the rectification behavior for PIn synthesized by microwave radiation but different oxidants is also different to each other. It may due to the difference in morphology and different dopants that affect mobility of the

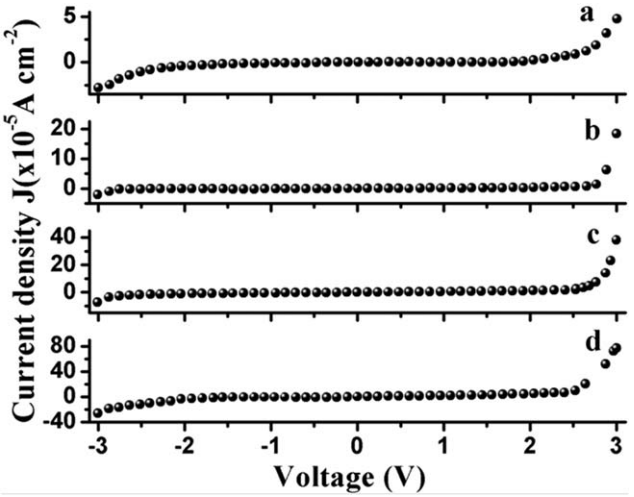

Figure 7. I–V characteristics of PIn formed by APS (a) and KIO_3 (b) (conventional synthesis), PIn formed by APS (c), and KIO_3 (d) (microwave synthesis).

Table III. Device Electrical Parameters

Synthesis method	Oxidizing agent	η	Φ_B (eV)	J_0 (A/cm ^{2})
Conventional	APS	4.66	0.88	1.39×10^{-8}
	KIO_3	5.02	0.73	8.36×10^{-8}
Microwave	APS	2.67	0.74	3.21×10^{-6}
	KIO_3	2.8	0.63	4.62×10^{-6}

charge carriers at metal-PIn junction.[42] Device parameters for all set of devices are calculated in accordance to standard emission-diffusion theory. As per this theory, the dependence of current density on voltage for metal-semiconductor rectifying contacts is given by:[43]

$$J = A^* T^2 \exp(-q\Phi_B/kT)\ [\exp(qV/\eta kT)-1]$$
$$\text{where } A^* T^2 \exp(-q\Phi_B/kT) = J_o$$

where A^* is effective Richardson constant with $A^* = 120$ A cm^{-2}K^{-2}, η is ideality factor (diode quality factor), J_0 is saturation current density without external biasing, T is absolute temperature, Φ_B is the barrier height, and k is Boltzmann constant. The ideality factor (η) and barrier height (Φ_B) are obtained from slope and reverse saturation current density respectively. The values of the ideality factor, barrier height, and reverse saturation current density (J_0) are listed in Table III. As illustrated from this table, the ideality factor of all devices is greater than one. In case of conducting polymers, it is reported that recombination of charges occurs via traps in the junction. However, in ideal diode, the recombination occurs through band to band in the bulk areas, not in the junction. For instance, the deviation of η from 1.0 to 2.0 is attributed to the carrier drift diffusion process and the Sah-Noyce-Shockley creation recombination process[44] while η greater than 2.0 attributed due to the trap-assisted tunneling,[45] carrier leakage,[46] and barrier inhomogeneity.[47] In view of this fact, η for Al/PIn/ITO device (using PIn synthesized via microwave irradiation) is lower than that of Al/PIn/ITO device (using PIn synthesized conventionally), indicating enhanced charge transport across the interface for microwave synthesized PIn. On the other hand the large value of J_0 for Al/PIn/ITO device (using PIn synthesized via microwave irradiation) is observed compared with Al/PIn/ITO device (using PIn synthesized conventionally). It is expected due to low depletion width that causes a possibility of tunneling at the interface.[43]

The charge transport mechanism in the Schottky diode can also be understood by the ln-ln plot of J–V characteristics as shown in Figure 8. There are three linear sections, corresponding to three different charge conduction mechanisms. The first region (voltages up to 1.08 V) is due to an ohmic behavior while the second and third regions are mainly due to space charge limited current (SCLC) with an exponential distribution of traps in the band gap of the PIn material similar to that of polycarbazole as reported earlier.[48]

Similarly, the increase in J_0 and decrease in Φ_B, in case of PIn (synthesized via microwave irradiation), can be explained on

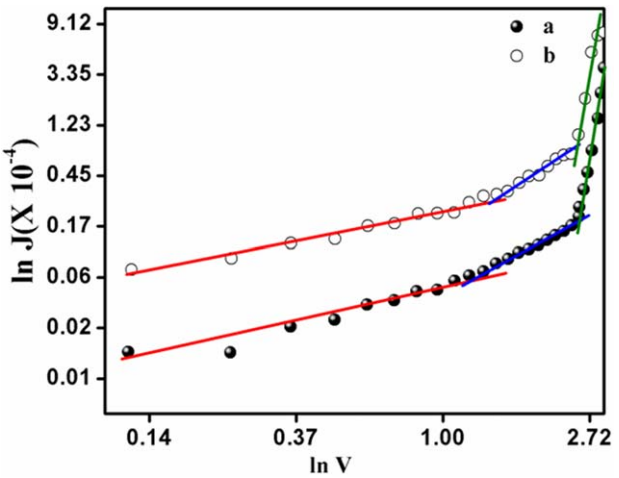

Figure 8. ln-ln plot of *J–V* characteristics of PIn formed from microwave synthesis method using (a) APS and (b) KIO_3. [Color figure can be viewed in the online issue, which is available at wileyonlinelibrary.com.]

the basis of surface morphology of polymeric chains as discussed earlier in SEM analysis section. The reduction in barrier height may be due to relatively smoother surfaces and interconnecting network (structure) of PIn (synthesized via microwave irradiation) compared with PIn (synthesized conventionally).[45] Conductivity measurement of the PIns is performed by four-probe method with the spin coated film of PIns. In this method, we measure conductivities at four different places on the film and average value of conductivity is shown in Supporting Information, Table S4. Similar trend of conductivity is observed as in the case of current densities measurement for device.

CONCLUSIONS

PIn is synthesized successfully using two different oxidizing agents, i.e., APS and KIO_3 and two techniques, i.e., conventional and microwave irradiation. We observed that in all the cases, PIn showed two to three fusion of individual monomer. PIn synthesized by APS (using either method) has better thermal stability compared with PIn synthesized by KIO_3 due to existing mixture of large and small fractions of polymeric chains. The Schottky device fabricated by PIn synthesized via microwave irradiation (APS and KIO_3) has better charge transport across the interface than other devices formed by PIn synthesized conventionally also confirmed by conductivity measurement. This is due to reduced barrier height and easier possibility of tunneling at the interface. This strategy of polymer synthesis can be extended for other polymers and also can be explored for various electronic applications.

ACKNOWLEDGMENTS

Madhu Tiwari is thankful to CSIR, New Delhi, India for JRF. Authors are thankful to Prof. M. A. Quraishi, Department of Chemistry, Indian Institute of Technology (Banaras Hindu University) for providing microwave facility and Prof. B. Ray, Department of Chemistry, Banaras Hindu University for GPC facility.

REFERENCES

1. Choi, S. J.; Kuwabara, J.; Kanbara, T. *ACS Sustain. Chem. Eng.* **2013**, *1*, 878.
2. Xu, S.; Luo, Z.; Han, Y.; Guo, J.; Wang, C. *RSC Adv.* **2012**, *2*, 2739.
3. Biswal, T.; Samal, R.; Sahoo, P. K. *J. Appl. Polym. Sci.* **2010**, *117*, 1837.
4. Adam, D. *Nature* **2003**, *421*, 571.
5. Landry, C. C.; Barron, A. R. *Science* **1993**, *260*, 1653.
6. Li, J.; Yi, X.; Lee, H.; Diddams, S. A.; Vahala, K. *J. Science* **2014**, *345*, 309.
7. Li, J.; Lee, H.; Vahala, K. *J. Nat. Commun.* **2013**, *4*, 2097.
8. Canadell, J.; Mantecon, A.; Cadiz, V. *J. Polym. Sci. Part A: Polym. Chem.* **2006**, *44*, 4722.
9. Hoogenboom, R.; Thijs, H. M. L.; Fijten, M. W. M.; Vanlankvelt, B. M.; Schubert, U. S. *J. Polym. Sci. Part A: Polym. Chem.* **2007**, *45*, 416.
10. Zhang, W.; Lu, P.; Wang, Z.; Ma, Y. *J. Polym. Sci. Part A: Polym. Chem.* **2013**, *51*, 1950.
11. Nagao, Y.; Takasu, A. *J. Polym. Sci. Part A: Polym. Chem.* **2010**, *48*, 4207.
12. Karnati, R.; Ford, W. T. *J. Polym. Sci. Part A: Polym. Chem.* **2008**, *46*, 3813.
13. Tiwari, M.; Gupta, S.; Prakash, R. *RSC Adv.* **2014**, *4*, 25675.
14. Kumar, A.; Pandey, A. C.; Prakash, R. *Catal. Sci. Technol.* **2012**, *2*, 2533.
15. Singh, A. K.; Singh, S. K.; Gupta, B. K.; Prakash, R.; Rai, S. B. *Dalton Transact.* **2013**, *42*, 1065.
16. Prakash, R.; Srivastava, R.; Pandey, P. *J. Solid State Electrochem.* **2002**, *6*, 203.
17. Reddy, K. R.; Jeong, H. M.; Lee, Y.; Raghu, A. V. *J. Polym. Sci. Part A: Polym. Chem.* **2010**, *48*, 1477.
18. Zhang, Y. P.; Lee, S. H.; Reddy, K. R.; Gopalan, A. I.; Lee, K. P. *J. Polym. Sci.* **2007**, *104*, 2743.
19. Reddy, K. R.; Lee, K. P.; Iyengar, A. G. *J. Polym. Sci.* **2007**, *104*, 4127.
20. Reddy, K. R.; Pilllee, K.; Gopalan, A. I.; Kim, M. S.; Showkat, A. M.; Nho, Y. C. *J. Polym. Sci. Part A: Polym. Chem.* **2006**, *44*, 3355.
21. Tiwari, S.; Singh, A. K.; Joshi, L.; Chakrabarti, P.; Takashima, W.; Kaneto, K. *Sens. Actuators B* **2012**, *171*, 962.
22. Reddy, K. R.; Lee, K. P.; Lee, Y.; Gopalan, A. I. *Mater. Lett.* **2008**, *62*, 1815.
23. Hnida, K. E.; Socha, R. P.; Sulka, G. D. *J. Phys. Chem. C* **2013**, *117*, 19382.
24. Kumar, A.; Prakash, R. *Chem. Phys. Lett.* **2011**, *511*, 77.
25. Nikolaidis, M. R. G.; Stanisavljev, D. R.; Easteal, A. J.; Zujovic, Z. D. *J. Phys. Chem. C* **2010**, *114*, 18790.
26. Riaz, U.; Ashraf, S. M.; Kumar, S.; Ahmad, I. *Chem. Eng. J.* **2014**, *241*, 259.
27. Riaz, U.; Ashraf, S. M.; Madan, A. *New J. Chem.* **2014**, *38*, 4219.

28. Tierney, S.; Heeney, M.; Mcculloch, I. *Synth. Met.* **2005**, *148*, 195.
29. Gupta, B.; Chauhan, D. S.; Prakash, R. *Mater. Chem. Phys.* **2010**, *120*, 625.
30. Gupta, B.; Prakash, R. *Synth. Met.* **2010**, *160*, 523.
31. Talbi, H.; Ghanbaja, J.; Billaud, D.; Humbert, B. *Polymer* **1997**, *38*, 2099.
32. Talbi, H.; Humbert, B; Billaud, D. *Synth. Met.* **1997**, *84*, 875.
33. Trznadel, M.; Pron, A.; Zagorska, M.; Chrzaszcz, R.; Pielichowski, M. *Macromolecules* **1998**, *31*, 5051.
34. Xu, J.; Hou, J.; Zhou, W.; Nie, G.; Pu, S.; Zhang, S. *Spectrochem. Acta A* **2006**, *63*, 723.
35. Joshi, L.; Gupta, B.; Prakash, R. *Thin Solid Films* **2010**, *519*, 218.
36. Nie, G.; Cai, T.; Zhang, S.; Bao, Q.; Xu, J. *Electrochem. Acta* **2007**, *52*, 7097.
37. An, S.; Abdiryim, T.; Ding, Y.; Nurulla, I. *Mater. Lett.* **2008**, *62*, 935.
38. Nikolaidis, M. R. G.; Stanisavljev, D. R.; Easteal, A. J.; Zujovic, Z. D. *J. Phys. Chem. C* **2010**, *114*, 18790.
39. Zettlemoyer, A. C. Nucleation; Dekker: New York, **1969**.
40. Davied, S.; Nicolau, Y. F.; Melis, F.; Revillon, A. *Synth. Met.* **1995**, *69*, 125.
41. Broido, A. *J. Polym. Sci. Part A: Gen. Pap.* **1969**, *7*, 1761.
42. Chung, S. F.; Wen, T. C.; Gopalan, A. *Mater. Sci. Eng. B* **2005**, *116*, 125.
43. Singh, A. K.; Joshi, L.; Gupta, B.; Kumar, A.; Prakash, R. *Synth. Met.* **2011**, *161*, 481.
44. Sah, C. T.; Noyce, R. N.; Shockley, W. *Proc IRE* **1957**, 45, 1228.
45. Casey, H. C. Jr.; Muth, J.; Krishnankutty, S.; Zavada, J. *M. Appl. Phys. Lett.* **1996**, *68*, 2867.
46. Rose, A. *Phys. Rev.* **1955**, *97*, 1538.
47. Forment, S.; Meirhaeghe, R. L. V.; Vrieze, A. D.; Strubbe, K.; Gomes, W. P. *Semicond. Sci. Technol.* **2001**, *16*, 975.
48. Pandey, R. K.; Singh, A. K.; Prakash, R. *AIP Adv.* **2013**, *3*, 122120.